geosciences

MDPI

Article

Numerical Modelling and Sensitivity Analysis of the Pitztal Valley Debris Flow Event

Mohammad Wasif Naqvi †, Diwakar Kc and Liangbo Hu *

Department of Civil and Environmental Engineering, University of Toledo, Toledo, OH 43606, USA; naqvimo1@msu.edu (M.W.N.); dibakarkc@outlook.com (D.K.)
* Correspondence: liangbo.hu@utoledo.edu
† Present address: Department of Civil and Environmental Engineering, Michigan State University, East Lansing, MI 48824, USA.

Abstract: Debris flows characterized by their rapid velocity and composition of water, mud, soil, and boulders, have the potential to inflict significant harm and present hazards to human life, infrastructure, and the natural surroundings. Numerical simulations provide a cost-effective approach for investigating different scenarios, hence boosting comprehension of flow dynamics and interactions. However, accurate modelling of these flows typically face difficult challenges arising from inherent modeling constraints and insufficient historical event data. The primary objective of the present study is to conduct numerical modeling and sensitivity analysis of the debris flow event that occurred in the Pitztal Valley, Austria in August of 2009, based on a multi-phase model for debris flows. The validation of the simulation results involves the comparison with the observed deposition patterns in the field. Various validation factors are employed to evaluate the accuracy of the simulated deposit and demonstrate a satisfactory level of precision in predicting deposition patterns. A sensitivity analysis is also conducted to examine the influence of in situ conditions on the effects of debris flow. The results demonstrate that numerical modelling can play an important role in engineering hazard assessment by analyzing the existing model's effectiveness in simulating both historical and projected debris flow events.

Keywords: geohazards; debris flow; debris deposition; numerical modelling; multi-phase

Citation: Naqvi, M.W.; Kc, D.; Hu, L. Numerical Modelling and Sensitivity Analysis of the Pitztal Valley Debris Flow Event. *Geosciences* **2023**, *13*, 378. https://doi.org/10.3390/geosciences13120378

Academic Editors: Jesus Martinez-Frias, Marco Cavalli, Chrysothemis Paraskevopoulou and Benoit Jones

Received: 1 October 2023
Revised: 26 November 2023
Accepted: 29 November 2023
Published: 11 December 2023

1. Introduction

Debris flows have long constituted a major threat to human life, settlement, environment and infrastructure [1–4], especially in the high mountain region. To mitigate the damages or fatalities caused by debris flow incident, understanding of flow characteristics and appropriate hazard assessments are needed for the delineation of hazard zones and the design of mitigation measures. Numerical modelling of debris flows offers a valuable approach for such purposes but typically requires validation and calibration of results based on available data of the past event. Various types of simulation models are often used for debris flow simulations. These models range from empirical-statistical approaches [5–8] to more physically based deterministic models based on rheology and flow behavior including single-phase dry granular flows [9–11] single-phase debris flows [12], mixture models [13,14], two-fluid models [15]. All these models effectively adopt a single-phase model for the material in motion and do not consider the effects of different interacting phases among the solid of different sizes and the fluid [16]. In the present study a multi-phase mass flow model developed by Pudasaini and Mergili [17] is explored. It incorporates several essential aspects of individual phases of flows related to their constitutive behavior, which allows the simulation of a variety of mass slides or flows [18] and is capable of unifying several widely used models [9,14,15].

A common challenge for all numerical modelling efforts remains the parameter calibration for assessing the capability and testing the performance of the model. It is preferable to conduct the model parameterization based on the well documented past events when relevant data were made available [19,20]. In the present study a back analysis of the debris flow event that took place in August 2009 in the Alpine region of Austria is performed to calibrate the relevant parameters used in the above-mentioned multi-phase flow model developed by Pudasaini and Mergili [17], including the frictional or resistance coefficients of multiple phases in motion. To assess the accuracy of the simulation, the validation is carried out by comparing the observed deposition pattern with the simulated deposition pattern, while quantitative validation scores are computed and analyzed. Subsequently a comparative sensitivity analysis is performed to analyze the impact of relevant modelling parameters.

2. Study Area

The study area investigated in the present study is located in the Pitztal Valley, southwest of Innsbruck, near the village of Plangeross, Tyrol, Austria (46°59′ N, 10°52′ E) (Figure 1). The catchment covers an area of approximately 0.7 km^2 and extends from 3343 m to 1620 m above sea level at the junction with the Pitze river. Approximately 70% of the area consists of gniess and mica schists as the bedrock and 30% of coarse talus deposits originated from the high alpine cirque. The debris overlying bedrock is present at the steep middle channelized part of the catchment, while a coarse debris flow material with large boulder size particles is present at the fan. A considerable part of the area is devoid of vegetation above the tree line in the upper part of the catchment which has high steep slopes (62° on average). The slope angle or gradient at the cone averages 30° and past debris flow deposits can be found primarily in the southern part of the channel [21,22].

The annual rainfall in the Pitztal valley varies between 600 and 11,500 mm/year based on the data collected at the gauging station located in Plangeross (1620 m above sea level). A well-documented debris flow event occurred in August 2009 with an approximate deposition of around 20,000–25,000 m^3 of material on the northers side of the fan (Figure 2). The event led to the blockage of the L16 road for several hours. This event is the main subject of the numerical modelling explored in the present study.

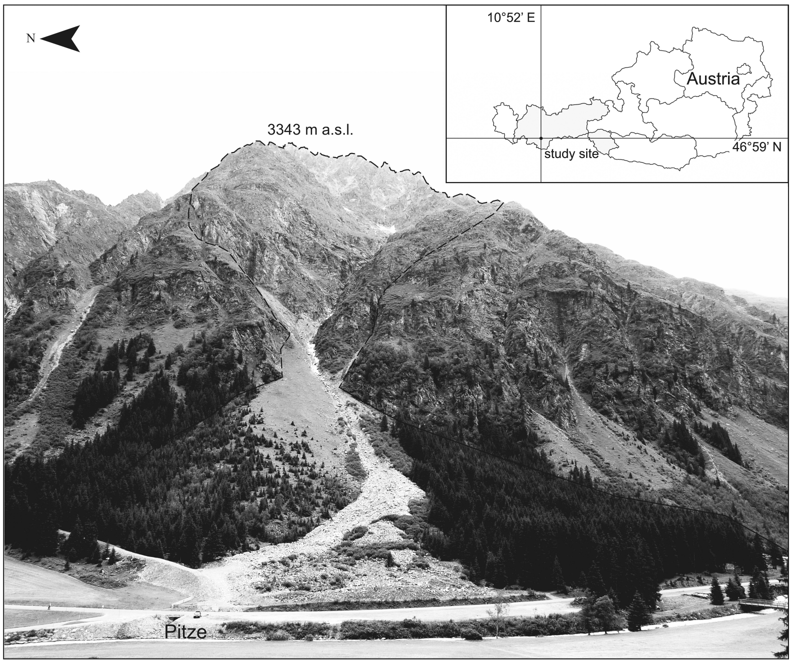

Figure 1. The study area in the Pitztal valley near the village of Plangeross, Austria. Reprinted with permission from [21], Taylor & Francis.

Figure 2. (**A**) A well-defined upper channel for material propagation; (**B**) the lower part of deposition with no apparent flow channel; and (**C**) an overall view of the post debris flow event of August 2009 in the Pitztal valley, Austria. Reprinted with permission from [21], Taylor & Francis.

3. Method

3.1. Numerical Modelling

In the present study the numerical modelling is based on a multi-phase mass flow model developed by Pudasaini and Mergili [17]. It expands the theoretical formulations of a two-phase (solid and fluid) model of Pudasaini [23] with the introduction of an additional phase of fine solid phase, thus allowing more complex material behavior to be considered in the modelling of the flow process. This multi-phase mass flow model incorporates the curvature effect of mountain topography, erosion and deposition mechanics and its subsequent effect on basal topography, in addition to the consideration of drag effects and virtual masses among different phases. The model is built upon a set of depth-averaged mass and momentum conservation equations for each of the three phases considered. The fluid phase is considered to be a mixture of water and very fine particles such as silt, colloids and clay. The latter are suspended in the water and their concentration may have an influence on the fluid yield strength [24,25]. It is modeled with shear-rate-dependent Herschel-Bulkley rheology. The fine solid phase contains fine gravel and sand. The rheology of this mixture is characterized by the rate-dependent visco-plastic behavior. The shear and pressure-dependent Coulomb viscoplasticity is adopted for this fine solid phase and both viscous stress and yield stress can significantly affect the behavior of fine solid. The solid phase is made up of boulders and coarser particles such as cobbles and gravels. These coarse particles are generally considered as frictional materials with no viscous contribution. The three phases are described by different material properties. The solid and fine solid phases are characterized by the material density, internal friction angle, the basal friction angle, an anisotropic stress distribution and the lateral earth pressure coefficient. The fine solid phase is also characterized by the its viscosity. The fluid phase is governed by the fluid density, viscosity and anisotropic stress distribution.

The mathematical model is implemented in an open-source computational package, r.avaflow 2.1 [20]. The package is supported by GIS for simulations of complex multi-phase mass flows over any arbitrary topographies. It is freely available as a raster module of the Geographic Resources Analysis Support System (GRASS) GIS software, Version 8.3 (Open Source Geospatial Foundation, USA) , employing the programming languages Python and C along with the statistical software R. In the present study the 5-m resolution Digital Elevation Model (DEM) data of the study area are retrieved from the openly available Austria database [26]. The data were originally generated using the Airborne laser scanning by the State government of Tyrol, Austria.

3.2. Modelling Background

A debris flow is a complex phenomenon [27–31] and its numerical modelling of a real-world event usually faces may difficulties and challenges, especially those related to often unknown material parameters and lack of data from the field measurements. The latter remains a most challenging task in almost every case study. In the present study the numerical modelling efforts are made to replicate the observation on this 2009 event in the study area and to provide the general overall characteristics of the event [21,22], although it should be acknowledged that there always remains a scope of improvisation and uncertainty.

Based on the observed deposit volumes and indication from aerial images, an initial release, in the form of mass block release (an instantaneous debris flow release), is provided with in initial height of 1.5 m and total volume of approximately 23,000 m^3. The solid fraction is assumed to be 0.85, which means a fluid fraction of 0.15 and a solid-fluid ratio of 0.85:0.15 in the back analysis of the event, based on the common fact that a large proportion of the debris flow are typically run off initiated [32,33] as well as the post-event field observation that the debris flow was primarily composed of large solid material. The presence of fine solid material is not invoked with its fraction set to be zero for the present simulations, because the numerical results based on the solid and fluid phases readily offer good match with the field observation, the presence of the fine solid phase would likely have little impact on the results in the present study.

The topography of the study region is presented in Figure 3 which also shows the flow path and the eventual debris deposition observed in the field. As mentioned in the preceding section, overall a considerable part of the mountain has very steep slopes of over 60°, as shown in Figure 4, which presents the elevation profile along the observed flow path from the west to the east. The initial trial simulation shows the debris material leaving the channel close to the fan and flowing towards the forest region, instead of flowing in the channelized path as was observed in the real event. To overcome this, a high value of ambient drag is assigned in the forest region, acting like a deflection wall, to restrict the flow in the channel. Sediment entrainment along the channel is not considered for the present study. The time step for output results generation is kept as 2 s.

Simulation results are presented in hydrographs which provide the flow height and the discharge. Three locations are selected to examine the evolution of the debris flow along its path: the first in the channel before the fan (marked as O1), the second at the start of the fan (O2), and the last at the L16 road (O3) in Figure 3. It is worth noting that the approximate deposition pattern remains the only reliable field data available [21], hence the numerical simulations are assessed based on the observed deposition pattern. Several key material parameters are calibrated based on the back analysis of this debris flow event, including the internal friction angle, the basal friction angle and the drag coefficient for the solid phase, as well as the kinematic viscosity and fluid friction coefficient for the fluid phase. Their values are determined based on the performance scores discussed in the subsequent section (Section 3.3). In addition, the density of solid is assumed based on the local rock presence; the density and the viscosity of fluid are assumed those of water, respectively.

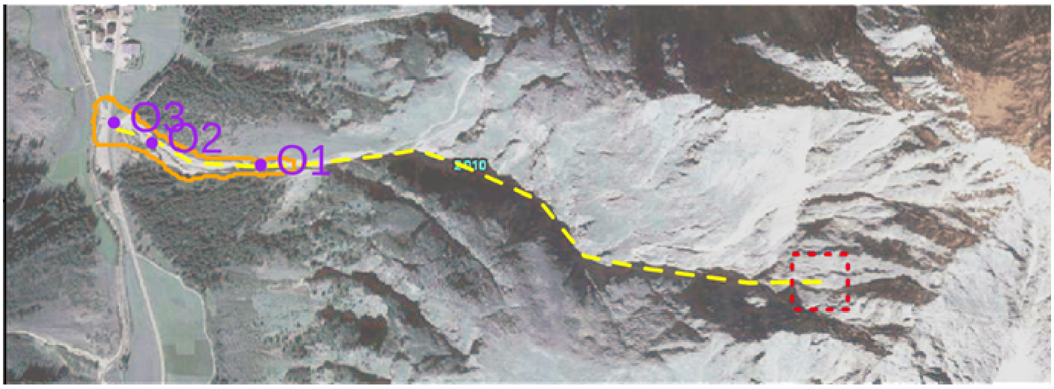

Figure 3. Topography of the study area of the Pitztal valley, Austrian. The red box indicates the initial release area, the yellow line the flow path and the orange area the observed deposit. O1, O2 and O3 denote the locations where the simulation results in the hydrographs are examined.

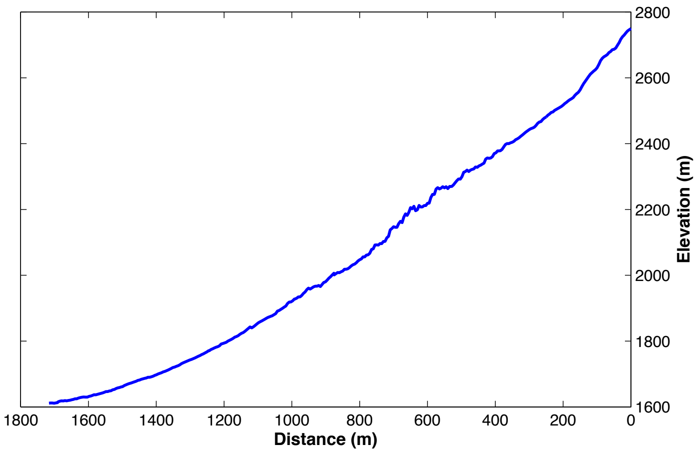

Figure 4. Elevation profile along the suspected flow channel of the debris flow event of August 2009 in the Pitztal valley, Austria. The horizontal origin is set up at the location of the debris initiation and the flow traveled towards the west (Figure 3).

3.3. Evaluation and Validation

In the present study several index parameters are used in the validation focusing on the comparison between the simulated deposit with the observed deposit. In the field observation [21], the pixels/cells/areas identified to be covered by debris deposition are referred to as observed positive (OP) while the celsl/areas with no deposit are termed as observed negative (ON). In a similar manner the numerical simulation results are examined by identifying the presence of debris deposition which is considered as predicted positive (PP), as well as the absence of debris deposition considered as predicted negative (PN).

Subsequently four validation outcomes associated with each cell can be readily established by comparing the observed with the simulated results: true positive (TP), false positive (FP), true negative (TN), and false negative (FN). TP represents the number of the cells observed with debris deposition and correctly predicted by the simulation, i.e., the intersection of OP and PP, while FP represents the number of the cells observed with no debris deposition but incorrectly predicted for its presence by the simulation (the intersection of ON and PP). Similarly, TN represents the number of the cells observed with no debris deposition and correctly predicted for its absence by the simulation (the intersection of ON and PN), while FN represents the number of the cells observed with debris deposition but incorrectly predicted for its absence by the simulation (the intersection of OP and PN).

In the present study four validation parameters based on these outcomes described [16,19,34], namely, critical success index (CSI), factor of conservativeness (FOC), Heidke skill score (HSS), and distance to perfect classification (D2PC), are assessed for the validation of the numerical modelling (Table 1). CSI and D2PC generally represent the degree of overlap between the observed and simulated deposit in the present study. CSI measures the performance of the model in correctly predicting the debris deposition relative to observed data. D2PC is a metric used to assess the accuracy of the prediction model that measures how far the model's predictions are from the ideal or perfect classification. A smaller distance indicates better model performance. HSS is a statistical measure that assesses the skill of a model in predicting categorical data, such as the occurrence or non-occurrence of deposition in the present study. It considers the model's performance relative to random chance, as a value of 1 indicates perfect skill, 0 no skill (similar to random chance) and negative values worse-than-random performance. FOC measures the conservativeness of the model in terms of its predictions. A model is considered conservative if it neither creates nor destroys mass or substance (i.e., deposition or non-deposition in the present study). For example, a value of 1 indicates perfect conservation, while values greater than or less than 1 indicate over-conservative or under-conservative behavior, respectively.

Table 1. Statistical parameters used in the assessment of the performance of the numerical modelling of the studied debris flow event. CSI measures the performance of the model in correctly predicting the debris deposition relative to observed data. FOC measures the conservativeness of the model in terms of its predictions. HSS is a statistical measure that assesses the skill of a model in predicting the occurrence or non-occurrence of deposition in the present study. D2PC is a metric used to assess the accuracy of the prediction model that measures how far the model's predictions are from the ideal or perfect classification.

Parameters	Definition	Range	Theoretical Optimum
Critical success index (CSI)	$CSI = \frac{TP}{TP+FP+FN}$	[0, 1]	1
Factor of conservativeness (FOC)	$FOC = \frac{TP+FP}{TP+FN}$	[0, ∞]	1
Heidke skill score (HSS)	$HSS = \frac{2\times(TP\cdot TN-FP\cdot FN)}{(TP+FN)(FN+TN)+(TP+FP)(FP+TN)}$	[−∞, 1]	1
Distance to perfect classification (D2PC)	$D2PC = \sqrt{(1-\gamma_{TP})^2+\gamma_{FP}^2}$ $\gamma_{TP} = TP/OP; \gamma_{FP} = FP/ON$	[0, 1]	0

3.4. Sensitivity Analysis

Sensitivity analysis is carried out to assess the effects of three key factors, the basal friction angle, the solid fraction and the initial volume of debris material. In each simulation while one of the three parameters is varied, all the other parameters are kept constant at their best fit values found in the back analysis of the event. In addition, a combination of two of the three key parameters are varied in additional simulations to generate and explore a wider range of the numerical results. Similarly to the back analysis, the observed deposition area is considered in the evaluation in the sensitivity analysis.

It is worth noting that all these three factors considered for sensitivity analysis vary in real life conditions and may have significant implications. The basal friction depends on the characteristics of bed material (i.e., size and shape), vegetation, concentration of sediments, and temperature [35]. The solid fraction can vary significantly and strongly influence the failure characteristics of the debris flow. Run-off generated failures generally have low solid concentration, while slope failure or earthquake generated debris flow are typically dominated by the solid proportion. Finally, many past studies [36–39] have reported the volume of landslide material ranging from hundreds to million cubic meter, it is of interest to examine its impact on the study area. For sensitivity analysis, the basal friction angle is varied from 1° to 20°, the solid fraction from 0.25 to 0.85, and the initial debris volume from 4500 to 60,000 m^3. It is worth noting that the best fit values used for these parameters in the back analysis are found to be 8°, 0.85 and 23,000 m^3, respectively.

4. Results and Discussion

4.1. Back-Analysis of the Event

Multiple trials of back-analysis are performed to calibrate relevant parameters that achieve high scores of the validation parameters as discussed in Section 3.3. Table 2 summarizes the final values of the parameters obtained that achieve the best performance in the simulations, including the internal friction angle (θ), the basal friction angle (δ) and the drag coefficient (λ) for the solid phase, as well as the kinematic viscosity (ν) and fluid friction coefficient (c) for the fluid phase.

Table 2. Material parameters of the solid and the fluid phases used for the back analysis of the studied debris flow event, Austria. The solid phase is primarily characterized by its density, internal friction angle, basal friction angle and drag coefficient, while the fluid phase by its density, viscosity and friction coefficient.

Parameter	Symbol	Value
	Solid	
Density	ρ_s	2840 kg/m^3
Internal Friction Angle	θ	35°
Basal Friction Angle	δ	8°
Drag Coefficient	λ	0.02
	Fluid	
Density	ρ_f	1000 kg/m^3
Kinematic Viscosity	ν	0.001 m^2/s
Fluid friction coefficient	c	0.08

It is worth noting that initial simulations indicate the flow of material moving to the left of the channel in the forest region, rather than in the direction of forest as observed in the field and also in previous study employing RAAMS-DF and DAN3D models [22]. In the subsequent simulations, to restrict the flow moving toward the forest region, a higher value of ambient drag of 10, is assigned in the forest region to force material towards the channel, while the normal value is used for the rest of the map.

Figure 5 shows the final simulated deposition which is consistent with the actual observed deposition. It is important to note that a previous study by Schraml et al. [22] employed the runout distance as a criterion for evaluating the model in the back analysis. In contrast, the present study utilizes the observed deposit as the primary criterion for model evaluation during the back analysis. In the former case an estimation of the debris flow initiation location was necessary which however is often challenging. Conversely, in the present study the deposition pattern can be discerned and proves to be a more effective model evaluation criterion. The three validation scores obtained in the back analysis are summarized in Table 3. The high scores of CSS and HSS reflect fairly good match of the simulation with the actual field observation. The simulated area mostly overlaps the observed deposition area. Considerable area turns out to be false positive (FP), hence the value of critical success index (CSI) is not very high. However, the factor of conservativeness (FOC) very close to its optimum value suggests very conservative results. The low value of the D2PC also indicates a good performance.

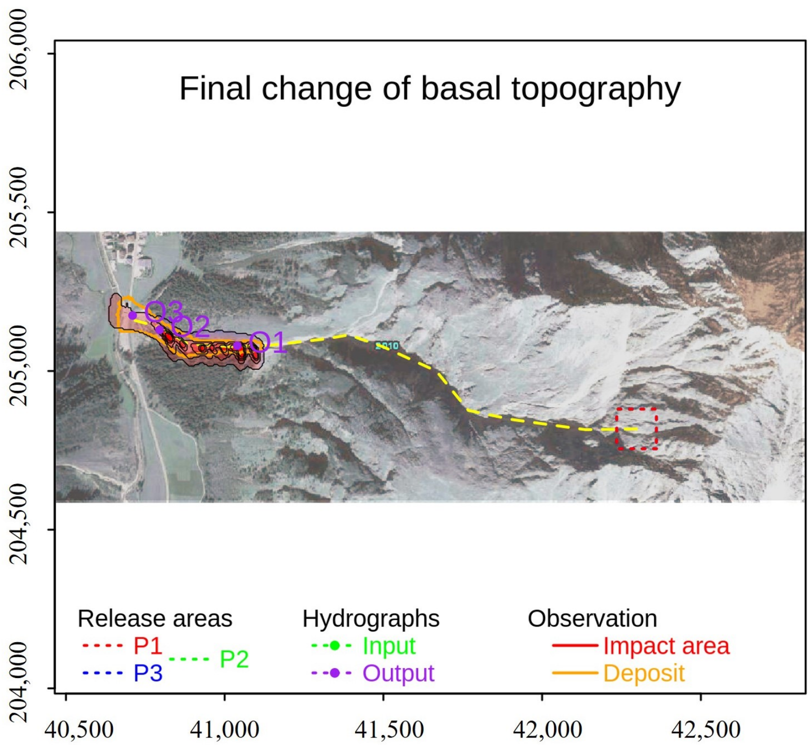

Figure 5. Final material deposition after the back analysis of the debris flow event of August 2009 in Pitztal valley, Austria.

Table 3. Summary of the values of the four statistical parameters obtained from the back analysis of the simulated debris flow event.

Validation Parameter	Value
CSS	0.464
FOC	1.004
HSS	0.574
D2PC	0.373

Other characteristics of the flow simulated can be also examined. The hydrographs at three selected locations discussed in Section 3.2 are presented in Figure 6, which show the height of flow and the discharge of the individual phases during the flow. A very high discharge of 240.85 m^3/s including solid and fluid phase, occurs at O1, located at the channel right before the fan due to a narrow channel and the high flow velocity. The discharge is then significantly reduced at O2 due to the high lateral spreading of material. This is consistent with the field record that a considerable amount of material was found on the road after the debris flow event. The simulation also shows a discharge of 29.87 m^3/s on the road and height of flow of 0.29 m (Figure 6c). The maximum total height of flow at O1 was 2.56 m with an individual height of 2.29 m and 0.27 m of solid and fluid phase, respectively (Figure 6a). Similarly, at O2 there is a total of 1.16 m of debris flow with 0.96 m of solid and 0.10 m of liquid (Figure 6b). The discharge at O2 is notably diminished as a result of the extensive lateral distribution of material. Figure 6b illustrates that the discharge at O2 is much smaller compared to O1. The data presented in Figure 6c indicates that there is material present on the L16 road at O3, as shown by the discharge and flow height.

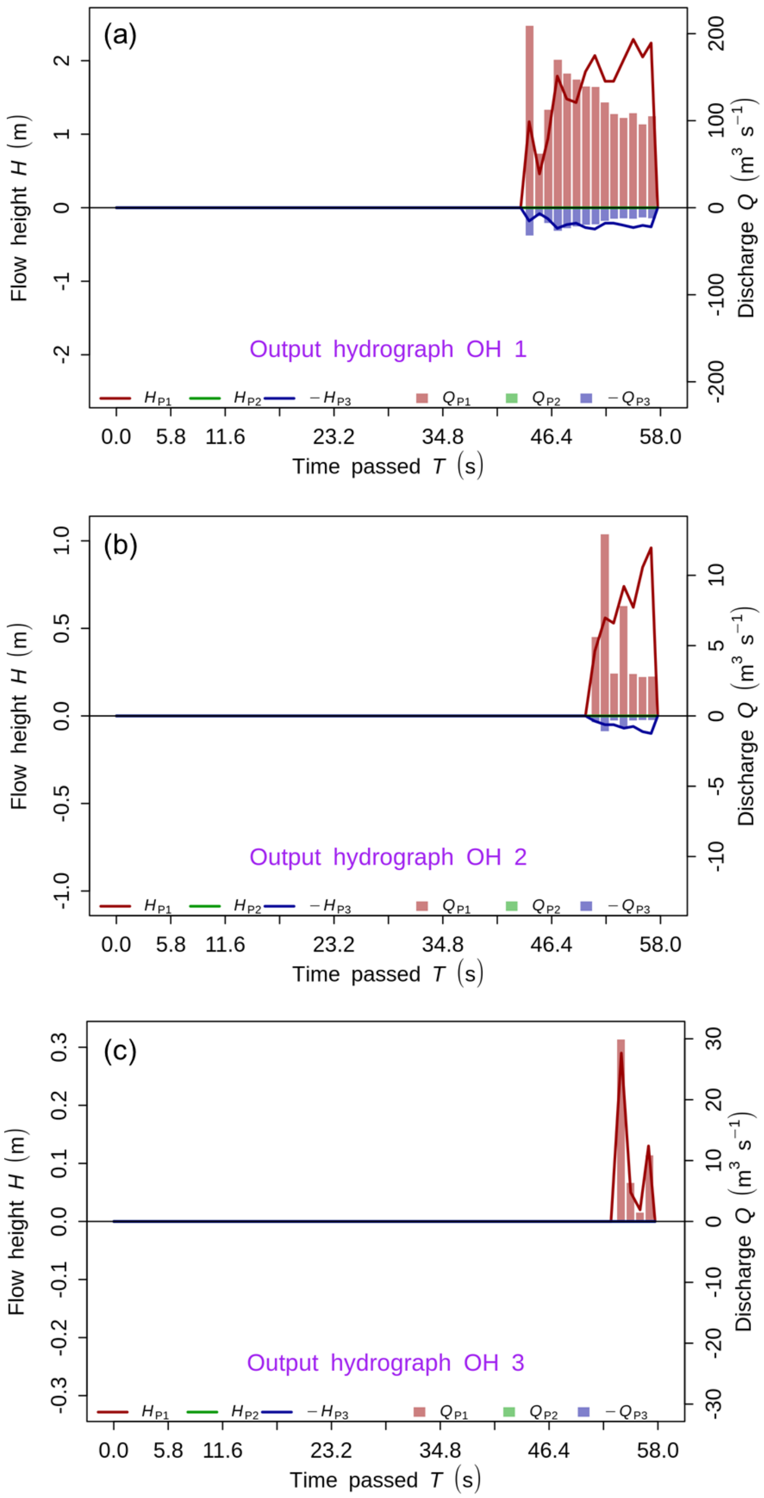

Figure 6. Hydrographs presenting the discharge rate and the flow height at the three marked locations, (**a**) O1, (**b**) O2 and (**c**) O3 along the flow path from the back analysis of the simulated debris flow event.

The maximum height of the debris flow along the flow path is another important parameter to examine. In the numerical simulation higher values of flow height are found in the upstream of the channel and in the center line of the flow path along the channel, as shown in Figure 7. At the location right after the release area, the values can often be over-predicted due to the block release as the majority of debris events are run-off initiated [40]. However, the effect of block release gradually declines with the distance. The maximum height of the flow in the range of 0.1 m to 3.8 is found at the fan and considerably decreased from its initial phase (Figure 7).

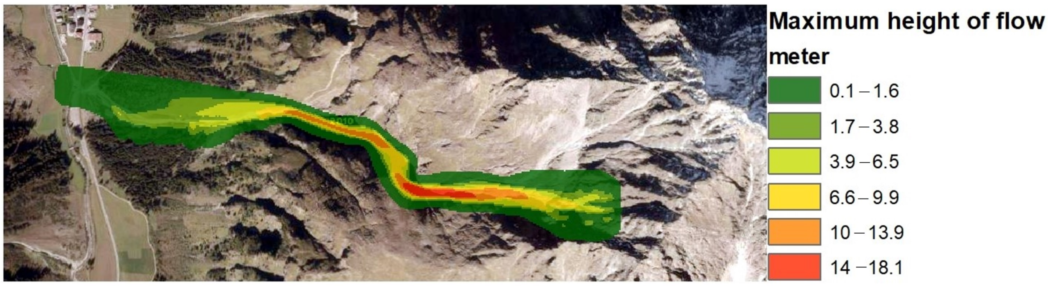

Figure 7. Maximum flow height along the flow path during the back analysis of the simulated debris flow event.

Figure 8 shows the maximum velocity of the flow in along its path. Generally the flow velocity reflects the severity and devastating momentum of any debris flow event. Velocities above 5 m/s are categorized as extremely rapid and pose a very high threat to communities due to no response time available [41]. The major factor controlling the velocity of flow is the gradient of the terrain. The maximum velocities in the numerical simulation reaches up to a value of 55 m/s. As mentioned in the section about the study area (Section 2), very high steep slopes of around 62° dominate in the upstream of the catchment and are the primary cause for such high velocities shown in Figure 8. The velocities decrease significantly in the fan region and a velocity in the range of 22–30 m/s is found at the L16 road. The time taken by the flow to reach the L16 road is approximately 57 s (Figure 9).

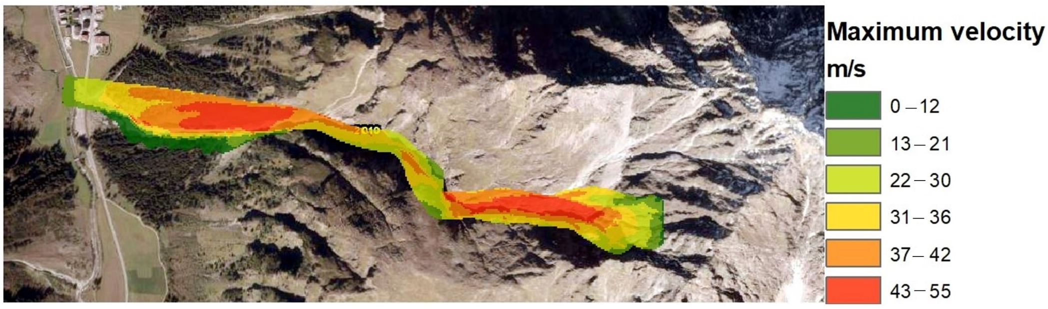

Figure 8. Maximum velocity of the flow along the flow path during the back analysis of the simulated debris flow event.

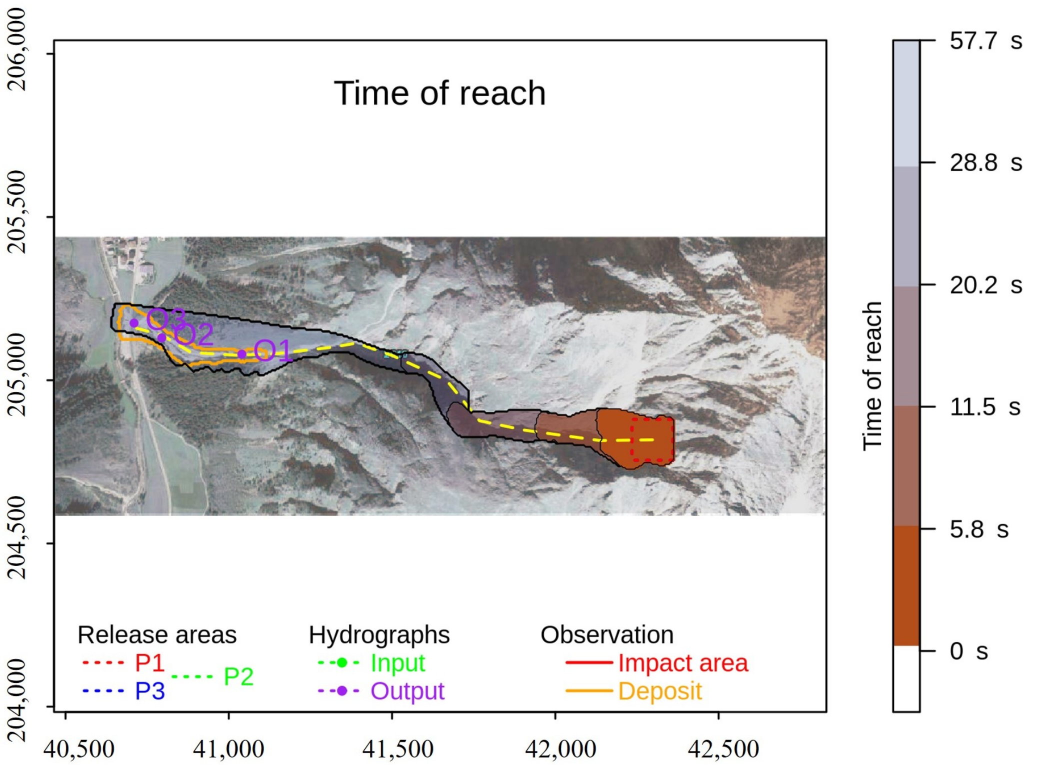

Figure 9. Travel time of the debris to reach any location along the flow path during the back analysis of the simulated debris flow event.

The kinetic energy and the flow pressure of the flow are also computed during the numerical simulation. The high magnitude of kinetic energy can be found in the upper part of the catchment and the value decreases subsequently as the flow moves down the hill towards the fan (Figure 10). The magnitude of the kinetic energy lies win the range of 0.13 MJ to 32 MJ. Similarly, Figure 11 presents the contour of maximum flow pressure. The maximum flow pressure is in the range of 0.07 to 19 MPa. The flow pressure in the range of 0.62 to 1.3 MPa can be found at L16 road. It is evident that the flow pressure builds up in the early part of its path after the initial release before it gradually declines possibly due to the frictional resistance, and finally grow considerably again near the deposition fan as the debris material accumulates there.

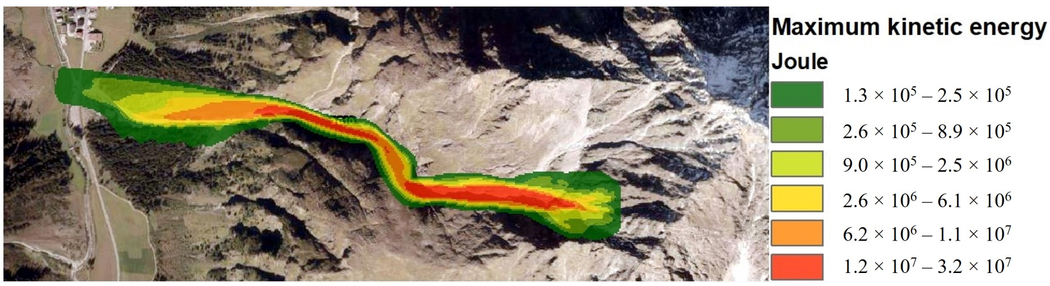

Figure 10. Maximum kinetic energy of the flow along the flow path during the back analysis of the simulated debris flow event.

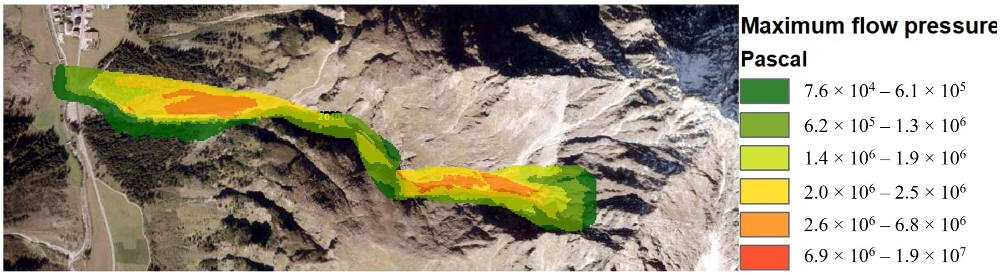

Figure 11. Maximum flow pressure of the flow along the flow path during the back analysis of the simulated debris flow event.

4.2. Results of the Sensitivity Analysis

In the sensitivity analysis the effects of three key factors, the basal friction angle (δ), the solid fraction (α) and the initial volume of debris material (V_m) are examined. Figure 12 shows the validation scores resulting from the sensitivity analysis when the basal friction angle (δ) and the solid fraction (α) are varied. CSI and HSS display their numerical optimum values for $\delta = 8^\circ \sim 12^\circ$ (Figure 12a) and $\alpha = 0.6 \sim 0.7$ (Figure 12c). For the solid fluid ratio $\alpha < 0.5$, very low scores less than 0.4 are obtained irrespective of friction angle. For D2PC, its optimum values can be observed around $\delta = 8^\circ \sim 12^\circ$ and $\alpha = 0.5 \sim 0.7$ (Figure 12d). The optimum values of FOC can be seen around $\delta = 8^\circ \sim 12^\circ$ and $\alpha = 0.75 \sim 0.85$ (Figure 12b). At high values $\alpha > 0.5$ and $\delta > 12^\circ$, FOC values less than 1 are obtained, suggesting a reasonable prediction of simulated deposition that does not grossly overestimate the deposition.

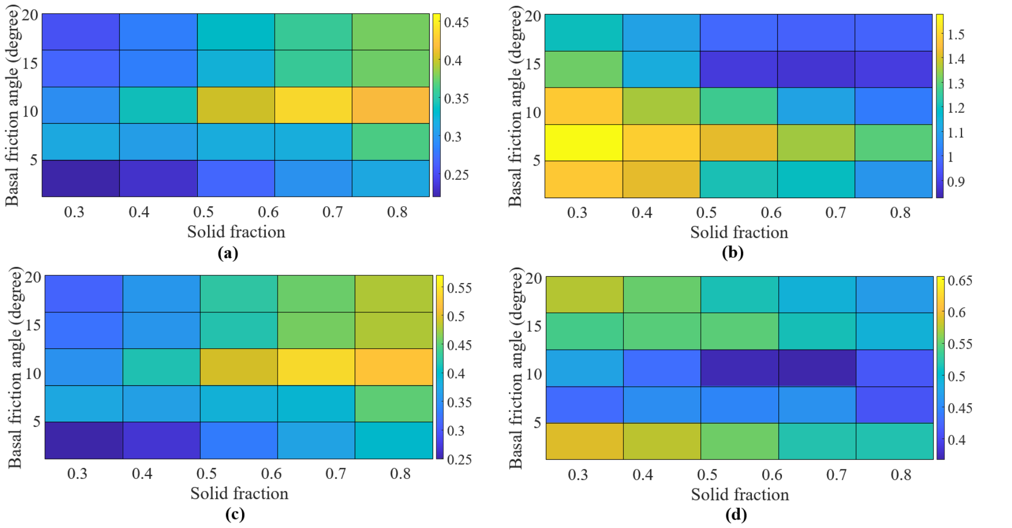

Figure 12. Validation scores including (**a**) Critical success index (CSI); (**b**) Factor of conservativeness (FOC); (**c**) Heidke skill score (HSS); and (**d**) Distance to perfect classification (D2PC) in the sensitivity analysis between basal friction angle and solid fraction.

Figure 13 shows the validation scores when the debris volume (V_m) is varied in conjunction with the varied basal friction angle (δ). The debris volume is a critical parameter that renders considerable influence on the amount of material moving along the flow path and eventual deposition [6,28,42], the results in these numerical simulations should be not directly compared with the field observation, but rather assessed within the sensitivity analysis. The CSS and HSS scores show similar distributions in a trend consistent with the previous case (Figure 12). It is worth noting that for cases with $\delta < 5$ and $V_m < 2000\ \text{m}^3$, the two scores obtained are lower than 0.3. It suggests that the numerical modeling would not adequately predict the observed deposit with the friction angle and the initial debris volume within these ranges. This seems also to lead to relatively poor D2PC scores as well. For the FOC, the optimum score is found for the volume range of 20,000 $\sim$ 45,000 m^3. Strong conservative results are obtained for the initial volume of greater than 45,000 m^3 while highly aggressive results are obtained for the volume of less than 20,000 m^3. It is evident that a large initial volume, in the range of over 20,000 m^3 in the numerical modeling would likely predict a deposition area that covers more of the actual field deposition.

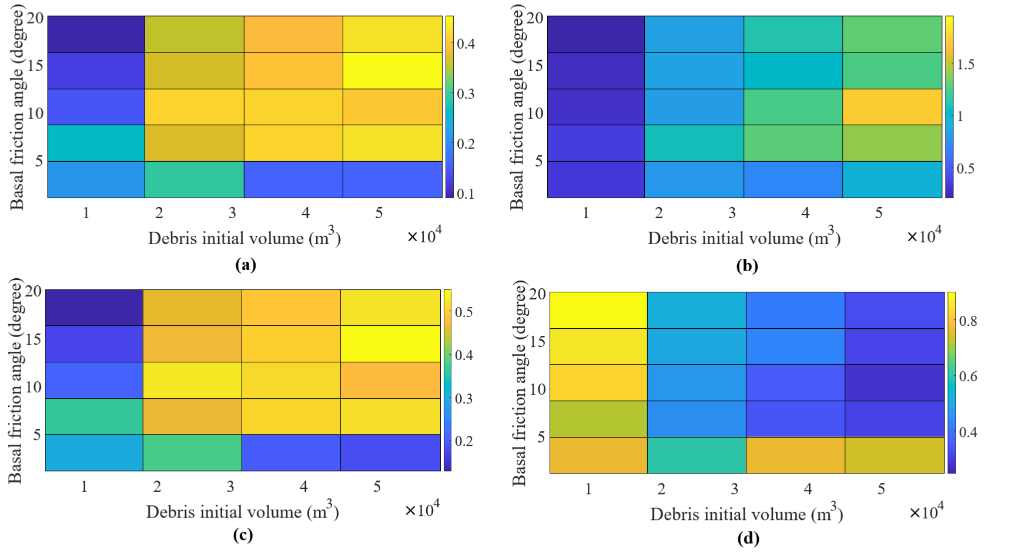

Figure 13. Validation parameter scores including (**a**) Critical success index (CSI); (**b**) Factor of conservativeness (FOC); (**c**) Heidke skill score (HSS); and (**d**) Distance to perfect classification (D2PC) in the sensitivity analysis between basal friction angle and initial debris volume.

The details of the final basal change in some cases with different modelling parameters can also be examined, including the following four cases, (a) the basal frictional angle $\delta = 5°$, (b) the fluid frictional angle $c = 0.01$, (c) the solid fraction $\alpha = 0.5$, and (d) the debris material volume $V_m = 50{,}000$ m^3, while all other parameters are kept identical to those in the back analysis. The results demonstrate the variations in deposition pattern by a slight change in the magnitude of the relevant parameters (Figure 14). For case (a), a low $\delta = 5°$ represents reduced roughness of the basal surface than the back-calibrated case of 8°, thus causing material to travel a longer distance than that in the back analysis. Similarly, in case (b), the low value of $c = 0.01$ also leads to a longer travel distance of the debris material than in the back analysis ($c = 0.08$); however, in this case the effect is less significant as the fluid friction parameter influences the effect of bed roughness on the fluid phase, as the fluid fraction is very small, i.e., less than 20% in the present study, thus the difference in travel distance is not remarkably different from the back analysis (Figure 5). For example, in case (c), there is a considerable greater presence of fluid phase than the back analysis ($\alpha = 0.15$), as the solid fraction $\alpha = 0.5$ indicates a debris rich in fluid phase and this provides easy mobility of the flow. Therefore, the final deposition area almost doubles the one observed in (Figure 5) for $\alpha = 0.85$. Finally, in case (d) when the initial volume is around 50,000 m^3 which is considerably higher than that in the back analysis, the flow travels the longest distance compared to other cases and the flow reaches the village area and poses a significant potential for damage and destruction.

The benefit of the numerical model lies in its capacity to simulate details and variations in debris flow dynamics based on the alterations in the key parameters. The examination of different scenarios provides valuable insights into the sensitivity of the model to changes in basal friction, fluid friction, solid fraction and debris volume. However, this subtle understanding comes with certain considerations and aspects that merit critical examination. First, while the model adeptly captures the influence of basal friction on debris flow behavior, the real-world scenario is likely more complex. In natural terrains, the basal surface may exhibit heterogeneous characteristics, and the model's assumption of uniformity might oversimplify the actual conditions. Secondly, the solid fraction may vary temporally due to the topography and dynamic behavior of flow, which could have an impact on the motion of the overall flow.

In essence, the presented model's ability to discern and quantify the impact of nuanced variations in modeling parameters leads to many subtle findings of the simulated event. The observed sensitivity to changes in basal roughness, fluid friction, solid fraction and debris volume highlights the model's robustness and its potential as a useful tool for assessing and understanding the complexities of debris flow events. However, while the presented numerical model offers valuable insights into the sensitivity of debris flow dynamics to various parameters, it is essential to approach the results critically. The model's performance in capturing real-world complexities should be continuously tested and refined through comprehensive validation against field data. Additionally, recognizing the simplifications and assumptions made in the model will benefit proper interpretation of its results in the context of actual debris flow events, fostering a more robust and reliable predictive tool for risk assessment and mitigation strategies.

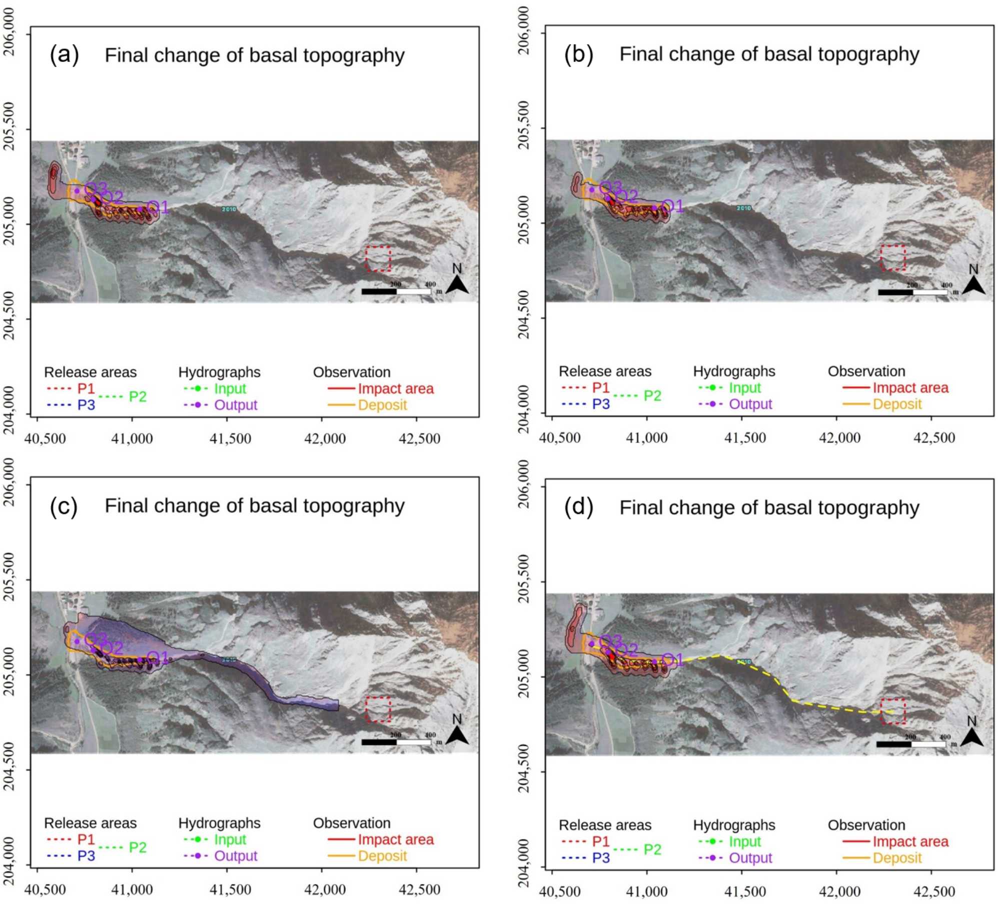

Figure 14. Final deposition pattern obtained from the sensitivity analysis by changing each material parameter individually, (**a**) the basal frictional angle $\delta = 5^\circ$, (**b**) the fluid frictional angle $c = 0.01$, (**c**) the solid fraction $\alpha = 0.5$ and (**d**) the initial debris volume $V_m = 50{,}000\ \mathrm{m}^3$.

5. Concluding Remarks

In the present study a debris flow event of August 2009 in Reiselehnrinne creek and Pitztal valley, Austria is analyzed based on a recently developed multi-phase flow model. Relevant modelling parameters are calibrated based on the field evidence of material deposition. The results are assessed using performance indicators including CSI, HSS, FOC and D2PC. These indicators yield respective values of 0.464, 1.004, 0.574, and 0.373, which collectively suggest a reasonably good degree of accuracy achieved in the simulation. The flow height, flow velocity, kinetic energy, flow pressure and peak discharge along the path of the debris flow are also simulated. The study estimated that the highest elevation of flow within the channel is 2.56 m, while it is 1.16 m at the beginning of the fan and declines to 0.28 m along the L16 road around the final debris deposition. The narrow channel sections exhibits a maximum flow velocity of 55 m/s, indicating a very high velocity and a great risk of potential damages. The time it takes for the debris to reach the L16 road is merely 57 s, which constitutes a very short period of time for human reaction facing the threat of the debris flow in motion. It is noted that there are two other major factors that may have significant influence of the model performance, including the availability of the DEM data of the actual topography which has a resolution of 5 m $\times$ 5 m for each cell, as well as the impact of the vegetation which cannot be directly considered in the numerical simulations. The cell size is larger than the channel width at some locations, makes it difficult to model accurately the flow characteristics. The influence of the vegetation is addressed by introducing a high value of ambient drag of the bed material in the forest region whose value is set up to be over 100 times that of the non-vegetated area, this leads to successful calibration of the material flow in the channel as observed.

The sensitivity analysis carried out clearly indicates the effect of bed roughness, solid-fluid ratio and initial debris volume on the behavior of the flow. The results are assessed through the four validation scores. While the model examined involves a number of flow parameters, the parameters, however, are not entirely arbitrary and can be estimated using existing field, experimental, or empirical data. Once properly calibrated, it allows extensive analysis on individual phases for case studies of past events and facilitates realizable prediction of the future events. The present study demonstrates the potential of numerical modelling that can be a useful tool in the simulation of past debris flow events and in the assessment of future hazard risks.

Author Contributions: Conceptualization, M.W.N.; methodology, M.W.N. and L.H.; software, M.W.N.; formal analysis, M.W.N.; investigation, M.W.N. and D.K.; resources, L.H.; data curation, M.W.N. and D.K.; writing—original draft preparation, M.W.N. and L.H.; writing—review and editing, L.H.; visualization, M.W.N. and D.K.; supervision, L.H.; project administration, L.H. All authors have read and agreed to the published version of the manuscript.

Funding: This research received no external funding.

Data Availability Statement: Data used in the present study is contained within the article.

Acknowledgments: The authors are grateful to Martin Mergili from University of Natural Resources and Life Sciences, Vienna, Austria, for assistance in the implementation of the numerical simulations with r.avaflow 2.1. The second author (D.KC) and third author (L.Hu) wish to acknowledge the financial support provided by the University of Toledo through a Summer Research Fellowship during the preparation of this manuscript.

Conflicts of Interest: The authors declare no conflict of interest.

References

1. Yune, C.Y.; Chae, Y.K.; Paik, J.; Kim, G.; Lee, S. W.; Seo, H.S. Debris flow in metropolitan area—2011 Seoul debris flow. *J. Mt. Sci.* **2013**, *10*, 199–206. [CrossRef]
2. Dowling, C.A.; Santi, P.M. Debris flows and their toll on human life: A global analysis of debris-flow fatalities from 1950 to 2011. *Nat. Hazard.* **2014**, *71*, 203–227. [CrossRef]
3. Ren, D. The devastating Zhouqu storm-triggered debris flow of August 2010: Likely causes and possible trends in a future warming climate. *J. Geophys. Res. Atmos.* **2014**, *119*, 3643–3662. [CrossRef]

4. Langdon, S.; Johnson, A.; Sharma, R. Debris flow syndrome: Injuries and outcomes after the Montecito debris flow. *Am. Surg.* **2019**, *85*, 1094–1098. [CrossRef] [PubMed]
5. Scheidegger, A.E. On the prediction of the reach and velocity of catastrophic landslides *Rock Mech.* **1973**, *5*, 231–236. [CrossRef]
6. Rickenmann, D. Empirical relationships for debris flows. *Nat. Hazard.* **1999**, *9*, 47–77. [CrossRef]
7. Legros, F. The mobility of long-runout landslides. *Eng. Geol.* **1999**, *63*, 301–331. [CrossRef]
8. Scheidl, C.; Dieter, R. Empirical prediction of debris-flow mobility and deposition on fans. *Earth Surf. Process. Landforms* **2010**, *35*, 157–173. [CrossRef]
9. Savage, S.B.; Hutter, K. The motion of a finite mass of granular material down a rough incline. *J. Fluid Mech.* **1989**, *199*, 177–215. [CrossRef]
10. Hungr, O. A model for the runout analysis of rapid flow slides, debris flows, and avalanches. *Can. Geotech. J.* **1995**, *32*, 610–623. [CrossRef]
11. Pudasaini, S.; Columban, H. Rapid shear flows of dry granular masses down curved and twisted channels. *J. Fluid Mech.* **2003**, *495*, 193–208. [CrossRef]
12. Bagnold, R.A. Experiments on a gravity-free dispersion of large solid spheres in a Newtonian fluid under shear. *Proc. R. Soc. Lond. Ser. Math. Phys. Sci.* **1954**, *225*, 49–63.
13. Voellmy, A. Uber die zerstorungskraft von lawinen. *Schweiz. Bauztg.* **1955**, *73*, 159–162.
14. Iverson, R.M.; Denlinger, R.P. Flow of variably fluidized granular masses across three-dimensional terrain. *J. Geophys. Res. Solid Earth* **2001**, *106*, 553–566.
15. Pitman, E.B.; Le, L. A two-fluid model for avalanche and debris flows. *Philos. Trans. R. Soc. Lond. Ser.* **2005**, *363*, 1573–1601. [CrossRef] [PubMed]
16. Mergili, M.; Fischer, J.T.; Krenn, J.; Pudasaini, S.P. r.avaflow v1, an advanced open-source computational framework for the propagation and interaction of two-phase mass flow. *Geosci. Model Dev.* **2017**, *10*, 553–569. [CrossRef]
17. Pudasaini, S.P.; Mergili, M. A multi-phase mass flow model. *J. Geophys. Res. Earth Surf.* **2019**, *124*, 2920–2942. [CrossRef]
18. Naqvi, M.W.; KC, D.; Hu, L. Numerical modeling and a parametric study of various mass flows based on a multi-phase computational framework. *Geotechnics* **2022**, *2*, 506–522. [CrossRef]
19. Mergili, M.; Bernhard, F.; Jan-Thomas, F.; Christian, H.; Shiva, P.P. Computationale experiments on the 1962 and 1970 landslide events at Huascaran (Peru) with r.Avaflow: Lessons learned for predictive mass flow simulations. *Geomorphology* **2018**, *322*, 15–28. [CrossRef]
20. Mergili, M.; Jaboyedoff, M.; Pullarello, J.; Pudasaini, S.P. Back calculation of the 2017 piz cengalo-bondo landslide cascade with r.avaflow: What we can do and what we can learn. *Nat. Hazards Earth Syst. Sci.* **2020**, *20*, 505–520. [CrossRef]
21. Kogelnig-Mayer, B.; Markus, S.; Michelle, S.B.; Johannes, H.; Florian, R.M. Possibilities and limitations of dendrogeomorphic time-series reconstructions on sites influenced by debris flows and frequent snow avalanche activity. *Arctic Antarct. Alp. Res.* **2011**, *43*, 649–658. [CrossRef]
22. Schraml, K.; Thomschitz, B.; McArdell, B.W.; Graf, C.; Kaitna, R. Modeling debris-flow runout patterns on two alpine fans with different dynamic simulation models. *Nat. Hazards Earth Syst. Sci.* **2015**, *15*, 1483–1492. [CrossRef]
23. Pudasaini, S.P. A general two-phase debris flow model. *J. Geophys. Res. Earth Surf.* **2012**, *117*. [CrossRef]
24. Pszonka, J.; Schulz, B.; Sala, D. Application of mineral liberation analysis (MLA) for investigations of grain size distribution in submarine density flow deposits. *Mar. Pet. Geol.* **2021**, *129*, 105109. [CrossRef]
25. Pszonka, J.; Schulz, B. SEM Automated Mineralogy applied for the quantification of mineral and textural sorting in submarine sediment gravity flows. *Gospod. Surowcami Miner. Miner. Resour. Manag.* **2022**, *38*, 105–131.
26. European Commission. The Official Portal for European Data. Available online: https://data.europa.eu/data/datasets/0454f5f3-1d8c-464e-847d-541901eb021a?locale=en (accessed on 15 January 2020).
27. Calligaris, C.; Zini, L.; Calligaris, C.; Zini, L. Debris flow phenomena: A short overview? In *Earth Sciences*; Dar, I.A., Ed.; Intechopen: London, UK, 2012; pp. 71–89.
28. Iverson, R.M. Debris flows: Behaviour and hazard assessment. *Geol. Today* **2014**, *30*, 15–20. [CrossRef]
29. Turnbull, B.; Bowman, E.T.; McElwaine, J.N. Debris flows: Experiments and modelling. *C.R. Phys.* **2015**, *16*, 86–96. [CrossRef]
30. Wang, Z.-Y.; Lee, J.H.W.; Melching, C.S. Debris flows and landslides. In *River Dynamics and Integrated River Management*; Springer: Berlin/Heidelberg, Germany, 2015; pp. 193–264.
31. Thouret, J.C.; Antoine, S.; Magill, C.; Ollier, C. Lahars and debris flows: Characteristics and impacts. *Earth Sci. Rev.* **2020**, *201*, 103003. [CrossRef]
32. Coe, J.A.; David, A.K.; Jonathan, W.G. Conditions for debris flows generated by runoff at Chalk Cliffs, central Colorado. *Geomorphology* **2008**, *96*, 270–297. [CrossRef]
33. Coe, J.A.; Jason, W.K.; Scott, W.M.; Dennis, M.S.; Thad, A.W. Chalk Creek Valley: Colorado's natural debris-flow laboratory. *GSA Field Guid.* **2010**, *18*, 95–117.
34. Formetta, G.; Giovanna, C.; Pasquale, V. Evaluating performance of simplified physically based models for shallow landslide susceptibility. *Hydrol. Earth Syst. Sci.* **2016**, *20*, 4585–4603. [CrossRef]
35. Simons, D.B.; Richardson, E.V. *The Effect of Bed Roughness on Depth-Discharge Relations in Alluvial Channels*; USGS Water Supply Paper 1498-E; USGS : Reston, VA, USA, 1962.

36. Giraud, R.E.; Castleton, J.J. *Estimation of Potential Debris-Flow Volumes for Centerville Canyon, Davis County, Utah*; Utah Geological Survey: Salt Lake City, UT, USA, 2009.
37. Walter, F.; Amann, F.; Kos, A.; Kenner, R.; Phillips, M.; de Preux, A.; Huss, M.; Tognacca, C.; Clinton, J.; Diehl, T.; et al. Direct observations of a three million cubic meter rock-slope collapse with almost immediate initiation of ensuing debris flows. *Geomorphology* **2000**, *351*, 106933. [CrossRef]
38. Diwakar, K.C.; Dangi, H.; Naqvi, M.W.; Kadel, S.; Hu, L.-B. Recurring landslides and debris flows near Kalli Village in the Lesser Himalayas of Western Nepal. *Geotech. Geol. Eng.* **2023**, *41*, 3151–3168. [CrossRef]
39. Rom, J.; Haas, F.; Hofmeister, F.; Fleischer, F.; Altmann, M.; Pfeiffer, M.; Heckmann, T.; Becht, M. Analysing the large-Scale debris flow event in July 2022 in Horlachtal, Austria using remote sensing and measurement data. *Geosciences* **2023**, *13*, 100. [CrossRef]
40. Kean, J.W.; McCoy, S.W.; Tucker, G.E.; Staley, D.M.; Coe, J.A. Runoff-generated debris flows: Observations and modeling of surge initiation, magnitude, and frequency. *J. Geophys. Res. Earth Surf.* **2013**, *118*, 2190–2207. [CrossRef]
41. Hungr, O.; Evans, S.G.; Bovis, M.J.; Hutchinson, J.N. A review of the classification of landslides of the flow type. *Environ. Eng. Geosci.* **2001**, *7*, 221–238. [CrossRef]
42. Iverson, R.M. The physics of debris flows. *Rev. Geophys.* **1997**, *35*, 245–296. [CrossRef]